PHILOSOPHICAL TRANSACTIONS B

rstb.royalsocietypublishing.org

Research

Cite this article: Gao M, Whitt JL, Huang S, Lee A, Mihalas S, Kirkwood A, Lee H-K. 2017 Experience-dependent homeostasis of 'noise' at inhibitory synapses preserves information coding in adult visual cortex. *Phil. Trans. R. Soc. B* **372**: 20160156.
http://dx.doi.org/10.1098/rstb.2016.0156

Accepted: 19 August 2016

One contribution of 16 to a discussion meeting issue 'Integrating Hebbian and homeostatic plasticity'.

Subject Areas:
neuroscience

Keywords:
homeostatic synaptic plasticity, miniature inhibitory postsynaptic current, cortical plasticity, inhibition, spontaneous release

Author for correspondence:
Hey-Kyoung Lee
e-mail: heykyounglee@jhu.edu

†The first three authors contributed equally this this study.
‡Present address: Division of Neurology, Barrow Neurological Institute, Pheonix, AZ 85013, USA.
§Co-corresponding authors.
¶Present address: Department of Neuroscience, Mind/Brain Institute, Johns Hopkins University, 3400 North Charles Street, Dunning Hall Room 348, Baltimore, MD 21218, USA.

Electronic supplementary material is available online at https://dx.doi.org/10.6084/m9.figshare.c.3588653.

THE ROYAL SOCIETY PUBLISHING

Experience-dependent homeostasis of 'noise' at inhibitory synapses preserves information coding in adult visual cortex

Ming Gao[1,†,‡], Jessica L. Whitt[1,†], Shiyong Huang[1,†], Angela Lee[3], Stefan Mihalas[4,§], Alfredo Kirkwood[1,§] and Hey-Kyoung Lee[1,2,§,¶]

[1]Solomon H. Snyder Department of Neuroscience, Zanvyl-Krieger Mind/Brain Institute, Johns Hopkins University, Baltimore, MD 21218, USA
[2]Kavli Neuroscience Discovery Institute, Johns Hopkins University, Baltimore, MD 21205, USA
[3]Department of Biology, University of Maryland, College Park, MD 20742, USA
[4]Allen Institute for Brain Science, Seattle, WA 98103, USA

SH, 0000-0003-2976-5798; H-KL, 0000-0002-5554-983X

Synapses are intrinsically 'noisy' in that neurotransmitter is occasionally released in the absence of an action potential. At inhibitory synapses, the frequency of action potential-independent release is orders of magnitude higher than that at excitatory synapses raising speculations that it may serve a function. Here we report that the frequency of action potential-independent inhibitory synaptic 'noise' (i.e. miniature inhibitory postsynaptic currents, mIPSCs) is highly regulated by sensory experience in visual cortex. Importantly, regulation of mIPSC frequency is so far the predominant form of functional plasticity at inhibitory synapses in adults during the refractory period for plasticity and is a locus of rapid non-genomic actions of oestrogen. Models predict that regulating the frequency of mIPSCs, together with the previously characterized synaptic scaling of miniature excitatory PSCs, allows homeostatic maintenance of both the mean and variance of inputs to a neuron, a necessary feature of probabilistic population codes. Furthermore, mIPSC frequency regulation allows preservation of the temporal profile of neural responses while homeostatically regulating the overall firing rate. Our results suggest that the control of inhibitory 'noise' allows adaptive maintenance of adult cortical function in tune with the sensory environment.

This article is part of the themed issue 'Integrating Hebbian and homeostatic plasticity'.

1. Introduction

Inhibitory synaptic transmission is critical for normal cortical functions. Indeed, dysregulation of inhibition has been implicated in many brain dysfunctions including mental disorders like schizophrenia [1] and autism [2]. In sensory cortices, strengthening of the functional connectivity between inhibitory interneurons and pyramidal cells dictate the maturation of cortical function [3]. The efficacy of inhibitory synaptic transmission can be quantified directly by recording action potential evoked inhibitory postsynaptic currents (eIPSCs), and also often assessed indirectly by measuring parameters of action potential-independent miniature inhibitory postsynaptic currents (mIPSCs). Changes in mIPSC amplitude have been used as indication of postsynaptic alterations, while mIPSC frequency changes have been attributed to altered presynaptic function or synapse number. However, recent evidence suggests that mIPSCs may arise from a different vesicle pool from those used for action potential evoked release [4–10], and that these pools use distinct molecular release machineries [6,8,9,11–13]. These observations hint at potentially independent control of these two modes of inhibitory synaptic transmission, which may serve different functions.

It is well documented that eIPSCs control the timing of neuronal firing with incoming activity [14,15], which is not only critical for proper information processing, but also for spike-timing dependent plasticity mechanisms [16]. While both eIPSCs and mIPSCs could affect neuronal responses via shunting, the potential function of action potential-independent mIPSCs themselves has remained largely speculative. It has been long recognized that the frequency of mIPSCs is normally very high across many brain regions [17,18] despite the fact that the density of inhibitory synapses is orders of magnitude less than that of excitatory synapses [19]. This observation has raised speculations that inhibitory 'noise' may serve a function [18]. In this study, we report that in adults visual experience specifically regulates inhibitory 'noise' (mIPSCs) without changing eIPSCs. In particular, visual experience reversibly regulates the frequency of mIPSCs, which is the only functional change in inhibitory synaptic transmission reported so far in adults during an age range previously referred to as the refractory period for plasticity [20]. Furthermore, we also found that non-genomic actions of oestrogen specifically alter mIPSC frequency in adult visual cortex, which suggests that this mechanism is a convergent locus for controlling inhibition in the adult brain. Theoretical analysis suggests that homeostatic regulation of both inhibition and excitatory synaptic transmission is required for maintaining both the mean and the variance of synaptic inputs, which is critical for information coding [21]. We confirmed *in silico* and *ex vivo* that changes in eIPSCs affect the temporal aspect of the neural code in feed-forward inhibitory circuits, and a specific reduction in mIPSC frequency, together with previously reported homeostatic adaptation of excitatory synaptic transmission [17,22–24], is able to produce homeostasis of both the mean and the variance of input current without affecting the temporal representation.

2. Material and methods

(a) Manipulation of visual experience

Wild-type mice (C57BL6/J) were raised in a normally lighted environment (12 L : 12 D cycle; control, NR) or dark-exposed (DE) for the duration of 7 days initiated at postnatal day 35 (P35). DE mice were cared for using infrared vision goggles under dim infrared light. Some of the DE mice were taken out to the lighted environment for 1 day (1 dL), 3 days (3 dL) or 7 days (7d L) to study the effect of re-exposure to light. Only adult (greater than or equal to P35) male mice were used for the experiments, including the oestrogen studies. Exceptions are studies shown in the electronic supplementary material, figure S1 and S2, which have data from juvenile mice (both male and female) within the critical period for comparison (see the electronic supplementary material for details). All animal procedures followed the guidelines of the National Institutes of Health (NIH) and were approved by the Institutional Animal Care and Use Committees (IACUC) of the University of Maryland and the Johns Hopkins University.

(b) Preparation of visual cortical slices

Each mouse was deeply anaesthetized with isoflurane vapours, and euthanized by decapitation. The brain was rapidly removed and immersed in ice-cold dissection buffer (in mM: 212.7 sucrose, 2.6 KCl, 1.23 NaH_2PO_4, 26 $NaHCO_3$, 10 dextrose, 3 $MgCl_2$, 1 $CaCl_2$) saturated with 95% O_2/5% CO_2 mixture. Blocks of primary visual cortices were rapidly dissected and sectioned into 300-μm-thick coronal slices using a Vibratome 3000 plus microslicer (Ted Pella, Redding, CA, USA). The slices were gently transferred to a submersion holding chamber with artificial cerebral spinal fluid (ACSF (in mM): 124 NaCl, 5 KCl, 1.23 NaH_2PO4, 26 $NaHCO_3$, 10 dextrose, 1.5 $MgCl_2$, 2.5 $CaCl_2$) saturated with 95% O_2/5% CO_2, and recovered at room temperature for approximately 1 h before recording. All recordings were done at 30°C.

(c) Whole-cell recording of miniature inhibitory postsynaptic currents

The visual cortical slices were moved to a submersion-type recording chamber mounted on a stage of an upright microscope (E600 FN-1; Nikon, Japan) equipped with infrared oblique illumination. mIPSCs were recorded in L2/3 pyramidal cells in the presence of 1 μM TTX, 100 μM D,L-APV and 10 μM 2,3-dihydroxy-6-nitro-7-sulfamoyl-benzo[f]quinoxaline-2,3-dione (NBQX) and analysed with the Mini Analysis programme (Synaptosoft, Decatur, GA, USA). Intracellular recording solution that allows $GABA_A$-R mediated IPSCs to reverse at 0 mV [25] was used (in mM: 140 CsCl, 8 KCl, 10 EGTA, 10 HEPES and 10 QX-314 at a pH of 7.3). Cells were held at −80 mV to record mIPSCs using a Multiclamp 700B amplifier (Molecular Devices, Union City, CA, USA), digitized at 2 kHz by a data acquisition board (National Instruments, Austin, TX, USA), and acquired using a custom-made Igor Pro software (WaveMetrics, Lake Oswego, OR, USA). The threshold for detecting mIPSCs was set at three times the root mean square (RMS) noise. There was no significant difference in RMS noise between the experimental groups ($p > 0.2$). Cells showing a negative correlation between mIPSCs amplitude and rise time were excluded from analysis, as well as mIPSCs with greater than 5 ms rise time, because these potentially reflect dendritic filtering. From each experiment 350–500 consecutive events were considered for the determination of mIPSCs frequency, but highly superimposed events constituting 'bursts' (more than 2 events, inter-event-interval < 10 ms) were excluded from the measurement of amplitudes (300 non-burst events from each cell were used for average amplitude calculations). The decay time constant was calculated using the average of 150–200 well-isolated events. Only the cells and recording conditions that met the following criteria were studied: V_m −65 mV at break-in, input R 200 MΩ, series R 25 MΩ. Cells were discarded if input R or series R changed more than 15%. Junction potentials were typically about −10 mV, and were left uncompensated. TTX, bicuculline, D,L-APV and NBQX were purchased from Sigma/RBI (St. Louis, MO, USA). For oestrogen experiments, mIPSCs were recorded before and after 10 min application of 50 nM 17-β oestradiol (E2, Sigma) or selective agonists of oestrogen receptor-α (ERα), 200 nM propylpyrazole triol (PPT, Cayman Chemicals) or ERβ, 250 nM diarylpropionitrile (DPN, Tocris). To block acute effects of oestrogen, ERα antagonist 1,3-bis(4-hydroxyphenyl)-4-methyl-5[4-(2-piperidinylethoxy)phenol]-1*H*-pyrazole dihydrochloride (MPP, Tocris) was bath applied at a concentration of 10 μM to visual cortex slices taken from DE mice. mIPSC recordings were obtained from 10 to 55 min post-MPP incubation.

(d) Dual whole-cell recording of unitary inhibitory postsynaptic currents

G42 mice [26] in which green fluorescent protein (GFP) is expressed in parvalbumin (PV) interneurons were used to perform dual whole-cell recordings. Presynaptic fast-spiking PV-interneurons were held in the current-clamp mode and their firing properties were assessed by delivering 1000-ms depolarizing current steps (figure 2*a*). Postsynaptic pyramidal cells were identified based on their morphology and electrophysiological properties, and were recorded in voltage-clamp mode ($V_h = -60$ mV). Unitary IPSCs (uIPSCs) were evoked at connected PV to pyramidal

cells in V1 L2/3. Paired action potentials were induced by injecting depolarized current pulses (1.2 nA for 2 ms, 100 ms interval) to PV cells. Cells were not used for analysis if $V_{rest} > -60$ mV, series resistance > 25 MΩ, or if any of these parameters changed by 15% during data acquisition. The internal solution for current-clamp recordings contains (in mM): 130 K-gluconate, 10 KCl, 10 HEPES, 0.2 EGTA, 4 Mg·ATP, 0.5 Na_2·GTP and 10 Na_2·-phosphocreatine; for voltage-clamp recording (in mM): 120 CsCl, 8 NaCl, 2 EGTA, 10 HEPES, 5 QX-314, 4 Mg·ATP, 0.5 Na_2·GTP and 10 Na_2· phosphocreatine. For both solutions, pH values were adjusted to 7.2–7.4 and the osmolarity was 275–290 mOsm.

(e) Whole-cell recording of evoked inhibitory postsynaptic current

The eIPSCs were measured from V1 L2/3 pyramidal cells in response to stimulation through bipolar electrodes placed in L4 and L2/3. To isolate the eIPSCs component, 100 µM D,L-APV and 10 µM NBQX were added to the bath solution. The cells were held at −80 mV and eIPSCs were recorded with the same intracellular solution to that of mIPSCs. The interval of paired pulses was 100 ms, and the stimulus intensity for both L4 and L2/3 stimulation was increased until maximal amplitude was obtained for each. To recruit maximal eIPSC, both L4 and L2/3 inputs were stimulated simultaneously. For measuring acute oestrogen effects, eIPSCs (inter-stimulus interval = 200 ms) were recorded before and after 10 min application of 50 nM 17-β oestradiol (E2, Sigma).

(f) Modelling Fokker–Planck formalism

The responses of a population of neurons were calculated using the Fokker–Planck equation. The Fokker–Planck equation works under the assumption that individual synaptic inputs are weak [27,28]. The equation and the details of this calculation are provided in the electronic supplementary material.

(g) Simulation of a feed-forward circuit using miniature inhibitory and miniature excitatory postsynaptic current data

Recordings of frequency and amplitude of miniature excitatory postsynaptic current (mEPSC) and mIPSC from 15 NR and 16 DE visual cortical neurons were used to simulate input–output functions. A third, hypothetical condition is also simulated, in which the amplitude rather than the frequency of the mIPSC changes (DE_{amp}). The mIPSC parameters used for the simulation were from the current study (P28 NR and the age-matched 7dDE groups), while the mEPSC parameters were obtained from a separate set of experiments using P28 NR and 7dDE (from P21 to P28) mice. The recording conditions for mEPSCs were identical to our previous study [24]. All simulations were performed for leaky integrate and fire neurons with leak membrane conductance of 10 nS and a difference between resting and threshold membrane potential of 20 mV. To mimic an up-state, a constant external current is injected which asymptotically brings the membrane potential to 5 mV below threshold. Experimentally measured parameters were used for the simulations. All simulations in the control condition had a capacitance of 114 pF, time constant of the mEPSC decay of 2.83 ms and of mIPSC decay of 5.96 ms, while for DE the capacitance was 108 pF, time constant of mEPSC decay 2.74 ms and of mIPSC decay 5.96 ms. The average frequency and amplitude of mEPSCs and mIPSCs for each simulated cell were identical to those recorded. For the control NR condition, mEPSC frequency was 6.19 ± 0.47 Hz, amplitude was 10.33 ± 0.28 pA and mIPSC frequency was 12.82 ± 0.88 Hz, amplitude was 51.08 ± 2.46 pA. For the DE condition, the mEPSC frequency was 6.26 ± 0.58 Hz, amplitude was 12.34 ± 0.43 pA and mIPSC frequency was 6.55 ± 0.37 Hz, amplitude was 52.3 ± 2.31 pA. The amplitude values of mEPSC and mIPSC were converted to conductance values for running the simulations, though differences between conductance and current based simulations were minimal. The hypothetical DE_{amp} condition had identical values to the DE condition except for in each neuron the mIPSC frequency was doubled (13.1 ± 0.74 Hz) and the amplitude halved (26.15 ± 1.15 pA) to bring the mIPSC frequency in line with what is observed in the NR condition while maintaining, for each cell, total inhibitory current identical to the DE condition. To simulate input–output curves, additional EPSCs (representing eEPSCs) with amplitudes four times the recorded spontaneous mEPSC were distributed as a Poisson process with frequencies ranging from 0 to 6000 Hz. Each simulation was 0.1 s in length and repeated 100 times. The simulations were performed in MATLAB (MathWorks) using a fixed 0.1 ms time-step updating.

Besides simulations of isolated cells, a set of simulations designed to mimic a feed-forward inhibitory circuit was performed. For this, two populations (excitatory and inhibitory) of homogeneous neurons were simulated. These simulations have identical parameters to those of individual cells, but in addition to all the previously described inputs for individual cells an additional stereotypical inhibitory cell is simulated, designed to represent a small population of inhibitory neurons receiving feed-forward inputs identical to the excitatory neuron simulated and inhibiting it. These cells receive external inputs with the same distribution as the excitatory cell simulated; however, they will fire at higher rates due to lower capacitance: 17.92 pF. Its intrinsic noise comes from 19 pA mEPSCs at 14.5 Hz (data from S.H.) and 42 pA mIPSCs at 19 Hz (data from [29]). Upon firing, the stereotypical inhibitory cells produce eIPSCs in both the excitatory and inhibitory cells with a delay of 4 ms and 15 ms decay time constant, and they consist of a total of 10 release sites each with 0.3 release probabilities. For eEPSCs, four times the mEPSC amplitude was used based on approximate number of synaptic contacts between L4 and L2/3 pyramidal neurons [30]. These parameters result in a relatively balanced excitation/inhibition. The source code is available upon request.

(h) Playback of feed-forward simulation inputs

Whole-cell current-clamp recordings were done in L2/3 pyramidal neurons of NR mice using an internal solution for current-clamp recordings (the same as above). Excitatory and inhibitory synaptic transmission were pharmacologically blocked by adding 10 µM NBQX, 100 µM D,L-APV and 2.5 µM gabazine to the ACSF. The inputs of the feed-forward simulation were converted to current traces and played back to each neuron. Each neuron received 300 different input traces each simulating NR, DE and DE_{amp} conditions. Input current traces (100 ms each) were played back in blocks of 10 on a depolarizing current step to bring the membrane potential of the neuron to 5 mV below an action potential threshold, which was determined at the beginning of the experiment using a ramp current. A block of NR traces were followed by DE and subsequently by DE_{amp}, and repeated until all 300 traces for each condition were played back. Cells with input R 75 MΩ, series R 25 MΩ and V_{rest} −60 mV were used for the study, and cells showing greater than or equal to 15% drift in any of these parameters during the course of the recording were not used.

(i) Statistical analysis

For multi-group comparisons, one-factor analysis of variance (ANOVA) was used followed by Fisher's PLSD post hoc test or Newman–Keuls Multiple Comparison post hoc test to determine which group differs from each other. To determine interaction between two manipulations, a two-factor ANOVA was used. For two-group comparisons, unpaired and paired Student's *t*-tests

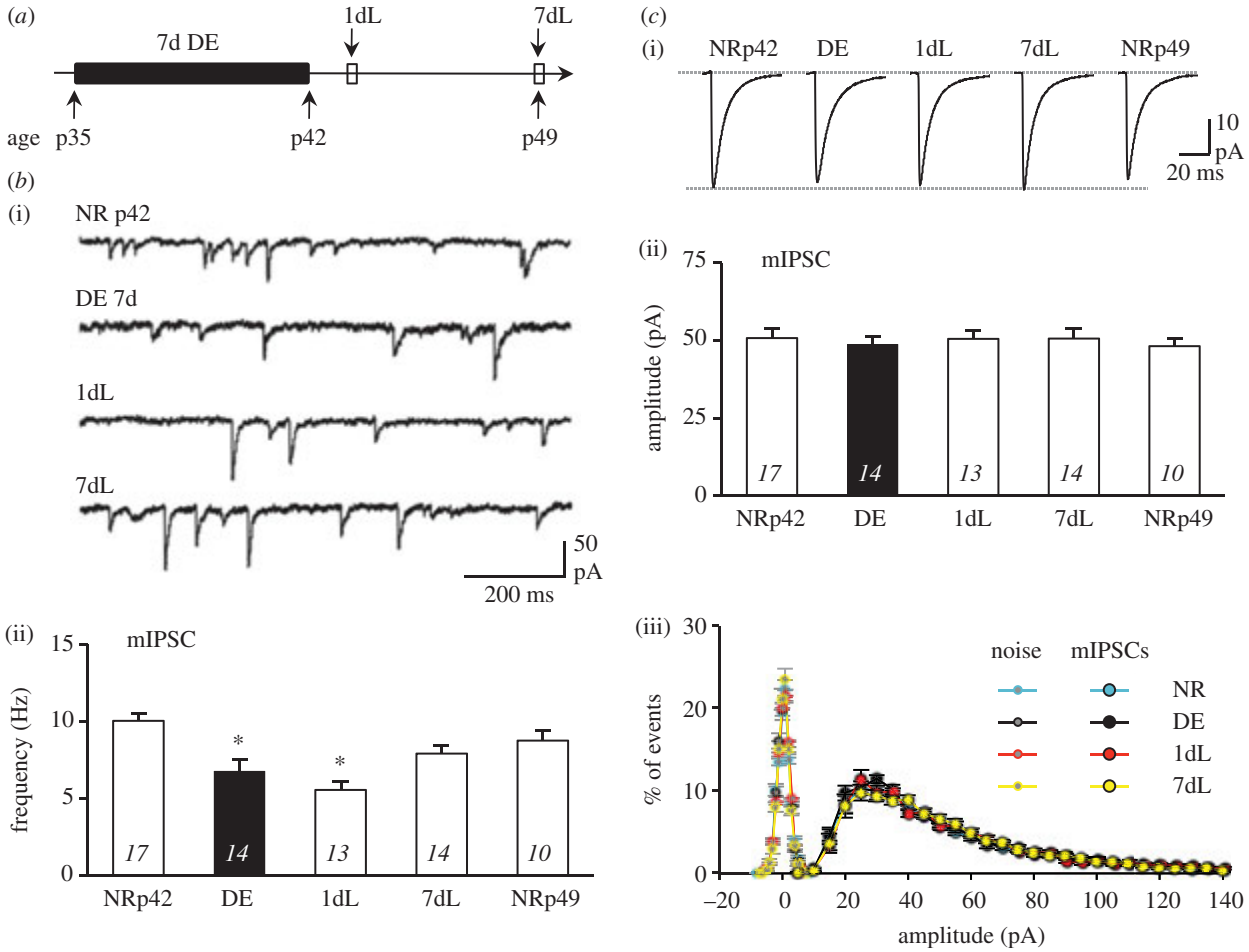

Figure 1. Visual experience reversibly alters mIPSC frequency in adults. (*a*) Experimental design. 7dDE was initiated at P35. (*b*) (i) Example mIPSC traces; (ii) 7dDE significantly decreased mIPSC frequency, which recovered with 7dL. (*c*) (i) average mIPSC traces; (ii) no change in average mIPSC amplitude across conditions; (iii) comparison of mIPSC amplitude distribution across groups. Distribution of baseline noise is plotted for each group to show clear separation of mIPSC amplitude from noise. The number of cells for each condition is indicated in each bar (*b*,*c*). *ANOVA, $p < 0.05$. For mIPSC parameters, see electronic supplementary material, table S1, see also figure S1.

were used as appropriate. For comparison of cumulative probabilities, the Kolmogrov–Smirnov test was used; $p < 0.05$ was taken as statistically significantly different.

3. Results

(a) Visual experience exclusively regulates miniature inhibitory postsynaptic current frequency in adults

It has been proposed, based on findings from *in vitro* systems, that the regulation of inhibition is essential for maintaining network homeostasis [31–34]. However, several studies have reported that inhibitory synaptic transmission in the visual cortex is malleable only during an early critical period, which ends around postnatal day 30–35 (P30–35) in the superficial layer neurons [25,35–37] and even earlier in the granular layer [38]. Following the critical period, visual cortical neurons exhibit a refractory period for inhibitory synaptic plasticity in adult rodents between P35 and P50 [20]. Therefore, we re-examined the issue of sensory experience-dependent plasticity of inhibitory synaptic transmission in the adult visual cortex during this refractory period. To do this, we visually deprived adult mice by placing them in a darkroom for one week (initiated at P35) following normal development with vision (figure 1*a*). We recorded mIPSCs as inward currents from layer 2/3 (L2/3) pyramidal neurons of the visual cortex by using symmetrical Cl^- gradient and recording at a negative holding potential. We found that a week of dark exposure (DE) significantly decreased the frequency of mIPSCs compared with normal reared (NR) controls in adults, and this gradually reversed with a week of light re-exposure (figure 1*b*). Experience-dependent regulation of mIPSC frequency was present at all ages examined (electronic supplementary material, figure S1*b*), which suggests that this mechanism is present throughout the critical period for ocular dominance plasticity and well into adulthood, even during the previously reported refractory period for inhibitory synaptic plasticity [20]. There was no significant change in mIPSC amplitude in adults after alterations in visual experience (figure 1*c*; electronic supplementary material, figure S1*a*). Neither was there a change in the parameters of $GABA_A$ receptor ($GABA_A$-R) function as deduced from peak-scaled non-stationary fluctuation analysis of mIPSCs (electronic supplementary material, figure S1*c*,*d*). The only effect on the amplitude of mIPSCs was observed when DE mice were re-exposed to light during the critical period, which we recently reported as a novel form of rebound potentiation of inhibition that depends on rapid transcription of brain-derived neurotrophic factor [37]. Our data indicate that the regulation of mIPSC amplitude and frequency can occur independently of each other, and that visual experience specifically controls mIPSC frequency in adults.

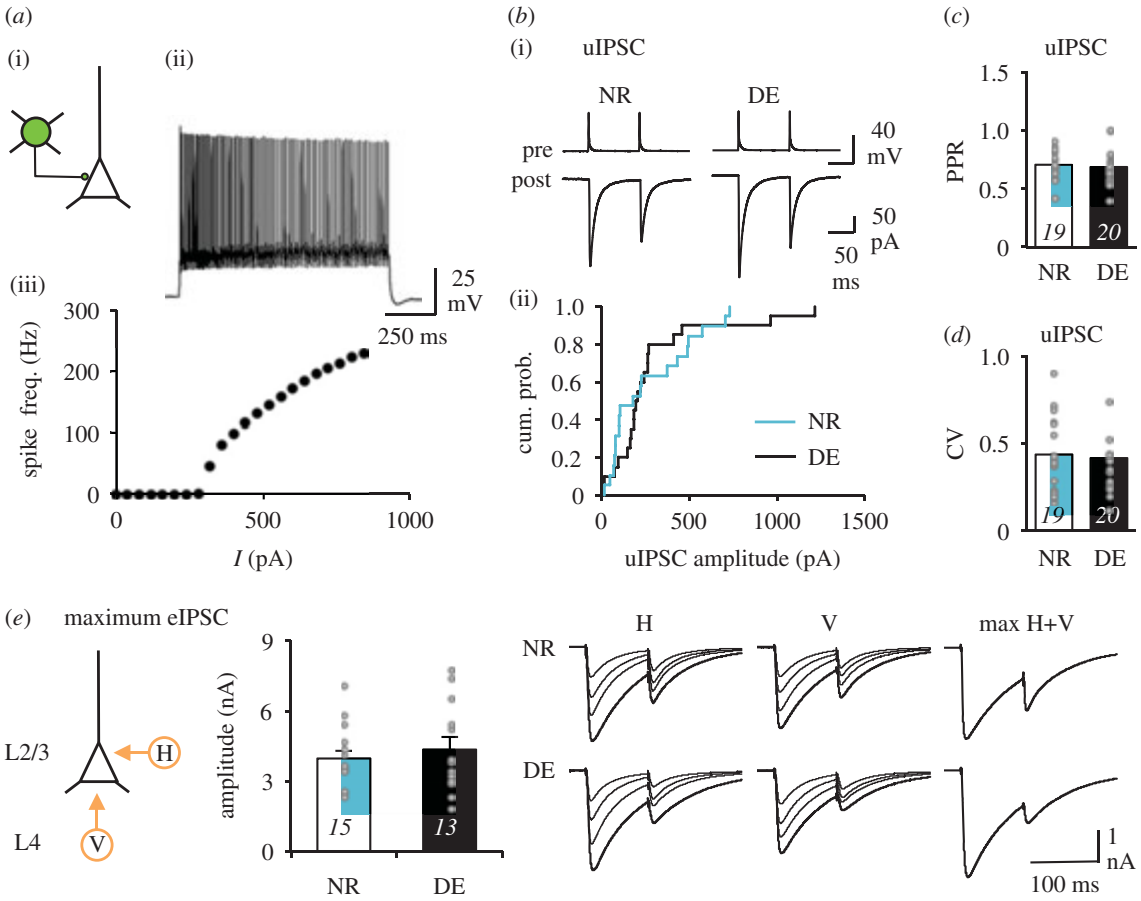

Figure 2. Absence of changes in uIPSC parameters or maximal eIPSCs in adults following visual deprivation. (*a*) (i) Schematics of paired recording between PV-interneuron and pyramidal cell. Consistent with many prior published studies, we verified that GFP-positive neurons in G42 mice are indeed fast spiking. (ii) An example current-clamp recording trace from a GFP-positive PV-interneuron upon 1-s depolarizing step current of 360 pA. (iii) Plot of action potential frequency evoked by 1-s depolarizing step current pulses of increasing amplitude. (*b*) (i) Average traces of presynaptic action potentials and postsynaptic uIPSCs from all cells for NR ($n = 19$ pairs) and DE ($n = 20$ pairs). The presynaptic PV neuron was stimulated at a 100 ms interval to obtain the paired pulse ratio (PPR). (ii) Cumulative probability of uIPSC amplitude comparison (Kolmogrov–Smirnov test: $p = 0.46$). There was also no significant change in PPR (*c*), CV (*d*) or failure rate (NR $= 0.08 \pm 0.03$, DE $= 0.07 \pm 0.03$) of uIPSCs (*t*-test, $p > 0.6$). (*e*) (i) Schematics of stimulating horizontal (H) and vertical (V) inhibitory inputs to a L2/3 pyramidal neuron; (ii) average maximum evoked IPSC (eIPSC) when both H and V pathways were simultaneously stimulated; (iii) example eIPSC traces for stimulation of H and V inputs (responses taken at 25%, 50%, 75% and 100% of maximum intensity are superimposed), and the maximum eIPSC when the two inputs were stimulated together at their respective maximum intensities (H+V). Two stimuli were given at a 100 ms interval for this experiment, but only the peak of the first response was analysed for comparison in the bar graph. There was no significant difference in the PPR measured at 50% maximum intensities (ANOVA, $p = 0.33$). The number of cell pairs or cells for each condition is indicated in each bar (*c*–*e*). (See also electronic supplementary material, figures S2–S4.)

The standard interpretation of alterations in mIPSC frequency is that there is either a change in synapse number or release probability, both of which would affect evoked inhibitory synaptic transmission. To examine this possibility, we first performed dual whole-cell recording in L2/3 from a pair of a synaptically connected parvalbumin (PV)-positive interneuron and a postsynaptic pyramidal neuron (figure 2*a*). We did not observe significant difference in the amplitude, paired pulse ratio (PPR), coefficient of variance (CV) or the failure rate of evoked uIPSCs across conditions (figure 2*b*–*d*). Similarly, we did not observe changes in presynaptic parameters of uIPSCs, such as PPR and CV, when DE was initiated during the critical period (electronic supplementary material, figure S2), which suggests that mIPSC frequency regulation is independent of presynaptic changes in eIPSCs across ages. Although the majority of recorded mIPSCs should reflect perisomatic synapses made by PV-positive neurons due to our rise time cut-off (see Material and methods) and similarity in kinetics (electronic supplementary material, figure S3), to rule out the possibility that the absence of changes in uIPSC parameters was due to limiting the presynaptic cell type, we simultaneously activated vertical (L4) and horizontal (L2/3) inputs to L2/3 pyramidal neurons to record maximal evoked IPSCs (eIPSCs). Again, there was no significant difference in the amplitude of maximal eIPSCs across NR and DE groups (figure 2*e*). Neither was there a change in PPR of eIPSCs measured at half maximum stimulation intensities, which suggests that experience-dependent regulation of mIPSC frequency occurred in the absence of changes in many of the parameters of eIPSCs. Furthermore, one week of DE initiated at P35 did not alter the density, size or intensity of GAD65 puncta (electronic supplementary material, figure S4), which suggests that DE at this age does not produce morphological changes to inhibitory synapses. Collectively, these results indicate that inhibitory synapses in the mature cortex respond to changes in visual experience mainly via reversibly controlling the frequency of mIPSCs. At present, this is the only form of functional plasticity at inhibitory synapses known to persist past the critical period and during the subsequent refractory period for plasticity.

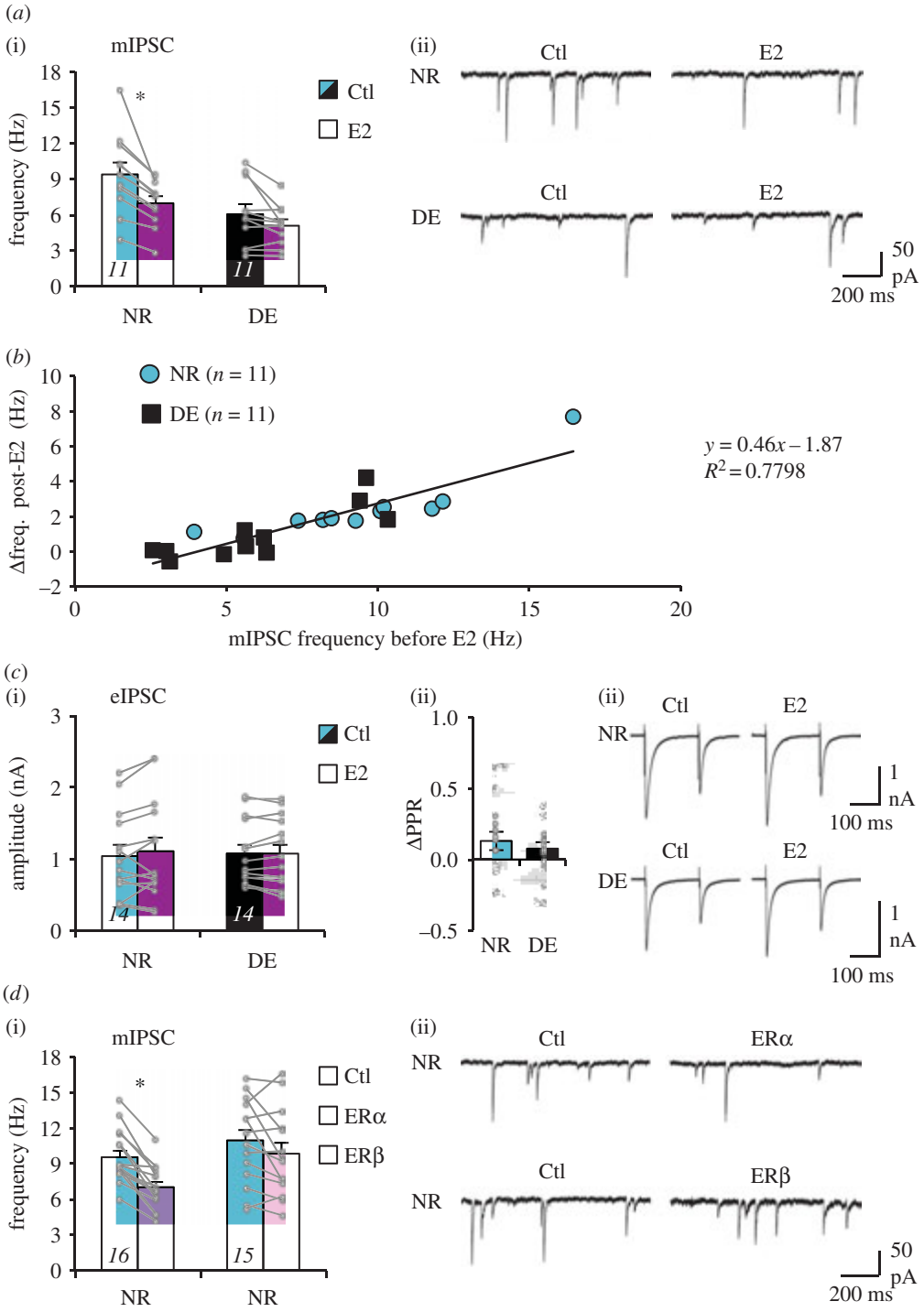

Figure 3. Oestrogen decreases mIPSC frequency without altering eIPSC parameters. (*a*) Acute application of 17-β oestradiol (E2, 50 nM for 10 min) significantly reduced mIPSC frequency in P42 NR mice, but not in mice with one week DE initiated at P35. (i) Comparison of averaged mIPSC frequency and (ii) example mIPSC traces before and after E2 application. There was no significant change in mIPSC amplitude (NR before E2 = 60 ± 7.5 pA, NR after E2 = 60 ± 7.0 pA, paired *t*-test: $p = 0.8$). (*b*) The magnitude of change in mIPSC frequency with E2 (Δfreq. post-E2) correlated with the initial frequency in each neuron. Equation for the linear fit and R^2-value are shown on the right. (*c*) Acute E2 did not alter eIPSC amplitude (paired *t*-test: NR, $p = 0.3$; DE, $p = 0.7$) or PPR measured with 200 ms ISI (paired *t*-test: NR, $p = 0.1$; DE, $p = 0.3$). (i) Comparison of average eIPSC amplitude; (ii) change in PPR (ΔPPR) with E2, calculated as ((PPR after E2) – (PPR before E2))/(PPR before E2); (iii) average eIPSC traces. (*d*) Acute application of agonist for ER-α (PPT, 200 nM), but not ER-β (DPN, 250 nM), reduced mIPSC frequency. (i) Average frequency comparison. Average across cells are shown as bars and average for individual cells before and after E2 are shown overlapped as grey circles connected with lines (*a*,*c*,*d*). Number of cells in each group is shown inside each bar. *$p < 0.001$, paired *t*-test. (ii) Example traces.

(b) Oestrogen rapidly regulates miniature inhibitory postsynaptic current frequency in adult visual cortex

Based on recent evidence that oestrogen is able to rapidly modulate inhibitory synaptic transmission in rat hippocampus via non-genomic actions [39], we examined whether oestrogen may target the same mechanism of mIPSC frequency regulation in the adult cortex by observing effects of acute oestrogen application on mIPSCs in L2/3 pyramidal neurons of male mice. We found that acute application of 17-β oestradiol (E2, 50 nM) for 10 min significantly reduced the frequency of mIPSCs recorded in NR P42 adults (figure 3*a*). By contrast, in one-week DE mice, which showed reduced mIPSC frequency compared with NR controls, there was no further decrease

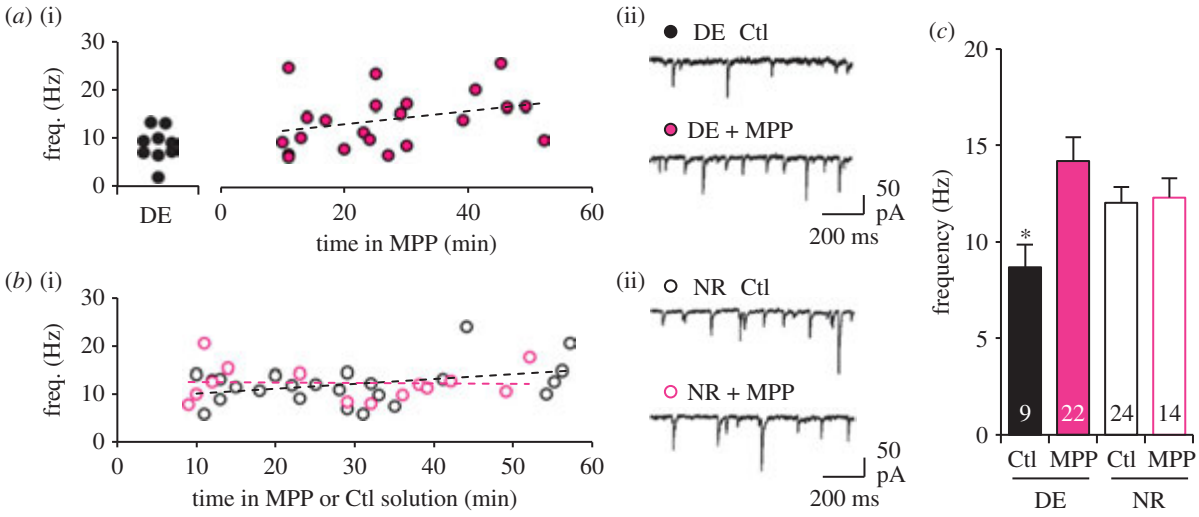

Figure 4. DE-induced reduction in mIPSC frequency is reversed by ER-α antagonist. (*a*) Acute application of ER-α antagonist (MPP, 10 μM) reversed the effect of DE on mIPSC frequency. (i) mIPSC frequency plotted for DE (DE Ctl: 8.7 $\pm$ 0.89 Hz, $n = 9$) and DE+MPP (14.2 $\pm$ 1.42 Hz, $n = 22$) conditions by incubation time. MPP significantly increased mIPSC frequency (*t*-test: $p < 0.005$) in a rapid manner, and there was no correlation between length of MPP incubation and mIPSC frequency ($R^2 = 0.09986$). (ii) Example mIPSC traces taken from a DE cell before and 12 min after MPP application. (*b*) Acute application of ER-α antagonist (MPP, 10 μM) did not alter mIPSC frequency in NR. (i) mIPSC frequency plotted for NR (NR Ctl: 12.3 $\pm$ 0.84 Hz, $n = 24$) and NR+MPP (12.3 $\pm$ 0.99 Hz, $n = 14$). The slopes of the linear regression lines fitted to NR Ctl and NR+MPP datasets were not statistically different from each other ($p > 0.05$). (ii) Example mIPSC traces. (*c*) Comparison of average mIPSC frequency across groups. There was statistically significant interaction between the rearing conditions and drug treatment (two-way ANOVA, $p < 0.002$). When comparing across groups, average mIPSC frequency of DE Ctl was statistically different (one-way ANOVA, $p < 0.001$; Newman–Keuls post hoc test, $^*p < 0.05$).

with acute E2 application (figure 3*a*). Acute E2 application did not alter the amplitude of mIPSCs in either NR or DE groups. Furthermore, the magnitude of mIPSC frequency decrease following E2 application was larger for neurons showing higher basal mIPSC frequency (figure 3*b*), which supports the idea that DE occludes the effects of E2. Our observation that prior DE occludes E2 effect suggests that acute oestrogen acts on the same downstream mechanism as DE to reduce mIPSC frequency. The effect of acute oestrogen was specific to mIPSCs, as we did not observe changes in the amplitude of eIPSCs from L4 to L2/3 pyramidal neurons before and after E2 application in NR or DE groups (figure 3*c*). Neither was there a change in PPR of eIPSCs after E2 application (figure 3*c*). These results suggest that acute E2 selectively decreases mIPSC frequency without affecting parameters of eIPSCs.

Oestrogen can exert rapid non-genomic action through two main receptors, oestrogen receptors alpha (ER-α) and beta (ER-β) [40]. Consistent with previous reports that ER-α is closely tied to the regulation of inhibitory synaptic function in rat hippocampus [39] and is located on presynaptic vesicles [41], acute application of ER-α selective agonist PPT (200 nM), but not ER-β agonist DPN (250 nM), for 10 min mimicked E2 by significantly reducing mIPSC frequency in P42 NR mice (figure 3*d*).

To test whether *de novo* oestrogen acting through ER-α plays a role in mediating the effects of dark exposure, we bath applied ER-α selective antagonist MPP (10 μM) to slices taken from male mice (P42) after one week DE. Acute application of MPP (10–55 min) reversed the effects of DE and increased mIPSC average frequency to control levels (figure 4*a*,*c*). The rapid effect of MPP (within 10–15 min) supports the idea that endogenous oestrogen exerts non-genomic actions in DE visual cortex. By contrast, application of MPP (10 μM) did not alter mIPSC frequency in age-matched male NR mice across time, which remained similar to that seen in control NR neurons recorded in vehicle solution (figure 4*b*,*c*).

Together these data indicate that oestrogen acutely acting through ER-α is able to reduce mIPSC frequency during DE, and suggest that oestrogen may preferentially act on vesicle pools associated with spontaneous release rather than evoked inhibitory transmission.

(c) Regulation of miniature inhibitory postsynaptic current frequency allows noise homeostasis in the context of a circuit

In addition to the alterations in mIPSC frequency that we describe here, visual deprivation also increases the strength of excitatory synapses [17,22,23,42,43]. In theory, the increase in the strength of individual excitatory synapses combined with reduction in input activity, due to visual deprivation, on their own could allow preservation of mean input current. However, potentiation of excitatory synaptic current will also increase the variance of the inputs. Several neuronal coding models assume that variance in responses, which is dependent on variance in the input, is an essential part of the information code [21]. Hence, to preserve information coding capabilities, it is crucial to preserve not only the mean input current, but also the variance of synaptic inputs. In order for homeostatic adaptation to preserve both the mean current and its variance, we propose that it requires plasticity at inhibitory synapses, in addition to the plasticity at excitatory synapses, as described below.

To establish the consequences for simultaneously controlling EPSC amplitude and mIPSC frequency, we used the Fokker–Planck equation to mathematically characterize the responses of a population of leaky integrate and fire neurons based on the mean and variance of the input currents. It represents a good approximation of neuronal dynamics if synapses are weak [27,28]. For the neuronal coding to be preserved between NR and DE conditions, both the drift and the

diffusion terms in the Fokker–Planck equation need to be equal across the two conditions. The drift term corresponds to the mean change in membrane potential caused by synaptic inputs (i.e. averaged input strength across time), while the diffusion term reflects the variance of the synaptic inputs (i.e. variability of inputs across time). As the charge carried by individual EPSCs increases following DE, a corresponding drop (about 15%) in the input frequency is required to preserve the total charge (see Material and methods for details). While such a change can sufficiently keep the mean synaptic charge (i.e. the drift) constant, it produces an increase in the variance of the synaptic inputs (i.e. the diffusion) due to larger fluctuations in membrane potential resulting from increased EPSC amplitude. Computationally, the variance of synaptic inputs can be kept constant following DE by reducing inhibition (see Material and methods). While controlling either mEPSCs or mIPSCs affects both the mean and the variance of synaptic inputs, there is a difference in relative contributions such that mEPSCs contribute more to the regulation of the mean and mIPSCs affect more the variance making their contributions linearly separable. Thus, a coordinated change in mEPSCs and mIPSCs is needed to maintain homeostasis of mean and variance in order to preserve neural coding.

Using the Fokker–Planck equation, we determined that regulation of inhibition is required to provide homeostasis of the variance of synaptic inputs (i.e. diffusion) as detailed below. All the parameters used in the calculation for NR and DE conditions were derived from experimental measures (see Material and methods). We also included a hypothetical condition of decreasing mIPSC amplitude instead of mIPSC frequency (DE_{amp} condition) to determine whether regulation of mIPSC frequency observed in our DE experiments has any differential functional consequence than altering inhibition via a postsynaptic mechanism. For DE_{amp} calculations, all the parameters were the same as in DE, but mIPSC amplitude was decreased instead of mIPSC frequency to match the total charge. In addition, eIPSC amplitude was proportionally decreased in the DE_{amp} condition, because postsynaptic regulation of $GABA_A$ receptors is predicted to change the amplitude of both mIPSCs and eIPSCs as we observe in juvenile mice [37] (electronic supplementary material, figure S2). We first applied the Fokker–Planck calculation to a single cell model. We observed that perfect homeostasis of synaptic variance cannot be achieved when mEPSCs are scaled up without concomitant downregulation of mIPSCs, but both DE and DE_{amp} conditions could do it (electronic supplementary material, figure S5 for details). By contrast, we found that selective regulation of mIPSC frequency is needed if the evoked inhibitory input frequency is also reduced in parallel to evoked excitatory inputs as is expected with visual deprivation. When we run the Fokker–Planck calculations using different inhibition levels (see the electronic supplementary material for details), we found that the diffusion term is better preserved by decreasing the frequency of mIPSCs (DE condition) rather than by reducing the amplitude of the mIPSCs (DE_{amp} condition) (electronic supplementary material, figure S5). Collectively, these results suggest that control of inhibition is crucial to maintain homeostasis of synaptic variance (i.e. drift), but selective regulation of mIPSC frequency is critical in the context of a circuit with evoked inhibition.

To further compare the functional consequences of changing the frequency of mIPSCs (DE) versus a hypothetical condition for decreasing the mIPSC amplitude (DE_{amp}) we ran simulations using a feed-forward inhibitory circuit model (figure 5). As with the calculation of Fokker–Planck equation, all of the parameters used to simulate the pyramidal neuron were derived from experimental measures (see Material and methods for details). To simulate a feed-forward inhibitory circuit, both the pyramidal neuron and an inhibitory neuron synapsing onto it received random Poisson distributed mEPSCs, mIPSCs, and additional eEPSCs at different frequencies (see Material and methods for details). In addition, when the inputs summate to reach the action potential threshold in the PV-interneuron, it triggered an eIPSC in the postsynaptic pyramidal neuron with a delay.

Decreasing the mIPSC frequency, combined with DE-induced scaling up of mEPSC amplitude [17,22–24,42], increased the input–output function of the simulated principal neuron (figure 5*a*), which is predicted by homeostatic adaptation to inactivity [44]. The hypothetical DE_{amp} condition similarly increased the input–output function at lower input activity, but more dramatically increased it at higher input activity (figure 5*a*), indicating that regulating the mIPSC frequency produces a milder change in the input–output function. By contrast, both DE and DE_{amp} conditions produced identical increases in the input–output function when simulated using an isolated neuron (electronic supplementary material, figure S6), which suggests that it is only in the context of a feed-forward inhibitory circuit that regulation of mIPSC frequency versus mIPSC amplitude makes a difference to neural activity. These results suggest that changing mIPSC amplitude has a larger impact on the gain of the circuitry than changes in mIPCS frequency. By contrast, we found that specific regulation of mIPSC frequency is better at providing noise homeostasis. In the same network model under the same conditions, we compared the Fano factor of neural responses, which is a measure of noise in postsynaptic spiking patterns. Consistent with the idea of noise homeostasis, the Fano factor of the DE group closely mirrored that of the NR group, which was pretty constant across a large range of inputs, while that of the DE_{amp} group deviated the farthest (electronic supplementary material, figure S7).

(d) Concomitant reduction in miniature inhibitory postsynaptic current frequency with scaled up mEPSCs better preserves the temporal profile of neuronal firing in the context of a circuit

Regulating mIPSC frequency may confer additional benefits by allowing selective control of action potential-independent inhibition without affecting eIPSCs. By contrast, postsynaptic regulation of $GABA_A$Rs likely impacts both forms of inhibitory synaptic transmission. To examine this, a 100-ms train of evoked excitatory inputs was given to the feed-forward inhibitory circuit and the resulting postsynaptic spike frequency was tabulated. Under control parameters (NR), postsynaptic spikes showed an initial phasic increase in frequency followed by a lower level tonic firing (figure 5*b*). This firing property is reminiscent of that observed in neurons of primary visual cortex upon presentation of oriented light bars [45–47]. We found that mIPSC frequency regulation (DE) preserves the temporal profile of neuronal firing to a train of inputs similar to the NR controls, while mIPSC amplitude regulation (DE_{amp}) does not because it increases the tonic firing rate (figure 5*b*).

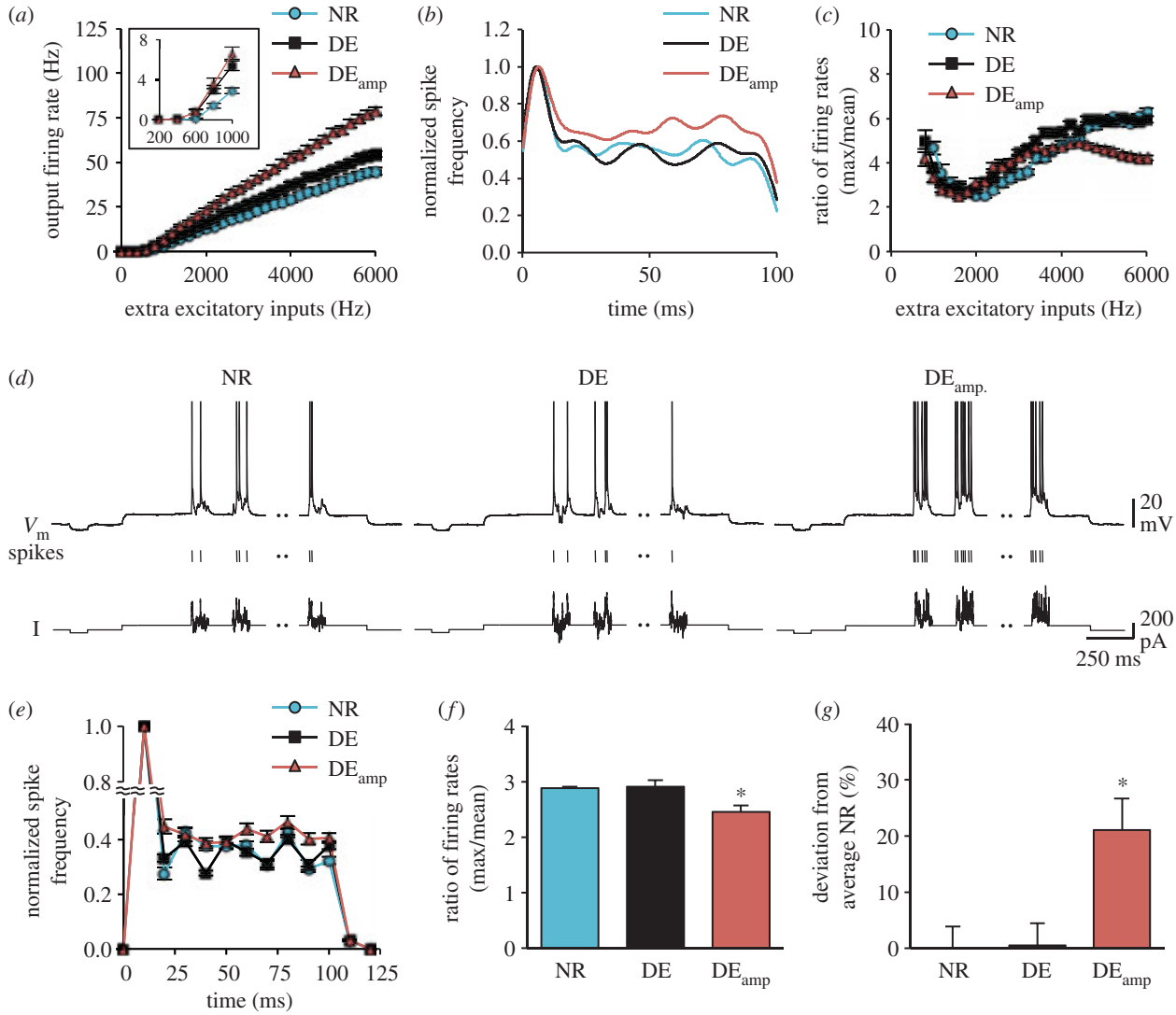

Figure 5. Regulation of mIPSC frequency in a local feed-forward inhibitory circuit preserves the temporal profile of neuronal responses while allowing homeostatic regulation of input–output function. (*a–c*) Simulation of a local feed-forward inhibitory circuit. (*a*) Comparison of input–output function of principal neurons receiving feed-forward excitation and inhibition with mEPSC and mIPSC parameters as measured for NR and DE groups. Data from P28 NR and 7dDE (from P21 to P28) were used for the simulation. The mIPSC data are from the current study (see electronic supplementary material, table S1 for the values), while the mEPSC data are from a separate set of experiments done using the same conditions. As reported previously, 7dDE significantly increased the average mEPSC amplitude without significant changes in mEPSC frequency (see Material and methods for the values). The input–output function increased in the DE condition compared with NR, which was milder than the result obtained with a hypothetical condition (DE$_{amp}$), where mIPSC amplitude was decreased, instead of frequency, to reduce the total inhibitory current to the same level as achieved by the reduction in mIPSC frequency seen under experimental conditions of the DE group. Inset shows the lower input range where both DE and DE$_{amp}$ show similar input–output function. (*b*) Comparison of an example of neuron response properties to a train of inputs (e.g. activation of 5000 inputs at 1 Hz). Neurons in a feed-forward circuit respond to a train of inputs by producing an initial high rate of phasic firing followed by a lower rate of tonic firing. The DE group produced similar response properties as the NR, while the hypothetical DE$_{amp}$ group produced a higher tonic firing rate. The responses are normalized to the maximum firing rate. (*c*) Average population responses: the difference in phasic and tonic firing to a train of inputs is quantified as maximum firing rate divided by the mean of tonic firing rate, and is compared across different number of inputs. The ratio of peak to plateau firing rate of DE$_{amp}$ is different from NR and DE conditions when the external input is sufficiently strong (e.g. more than 4000 inputs at 1 Hz). Thus the shape of the response signal is preserved by regulating mIPSC frequency as in DE, but is altered when inhibitory synaptic transmission is regulated postsynaptically (DE$_{amp}$). (*d–g*) Playback of simulation inputs to L2/3 pyramidal neurons of NR ($n = 14$ cells). (*d*) Example traces of the playback current traces (I) and the recorded postsynaptic responses (V_m). Spikes were detected using a threshold, and sorted into 10 ms bins to generate graphs shown in (*e–g*). Each neuron received 300 different 100-ms duration inputs for NR, DE and DE$_{amp}$ conditions used for the simulation, which were delivered on top of a depolarizing current step to mimic an up-state. (*e*) Normalized postsynaptic spiking frequency during the 100-ms stimulation epochs. DE$_{amp}$ stimulation resulted in a larger average firing rate during the tonic plateau phase (during 20–100 ms bins) compared with NR or DE (ANOVA, $p < 0.002$). (*f*) DE$_{amp}$ stimulation produced a significantly lower ratio of max-to-mean firing rate (*ANOVA, $p < 0.006$). (*g*) The normalized firing rate for each 10 ms bin during the tonic phase of DE$_{amp}$ significantly deviated from average NR values (*ANOVA, $p < 0.002$), which suggests less preservation of temporal firing profile (see also electronic supplementary material, figures S5–S8).

This was apparent at higher input frequencies, as shown with the ratio of postsynaptic action potential frequency during phasic (max) and tonic (mean) firing phases (figure 5*c*). Therefore, regulation of mIPSC frequency, rather than amplitude, allows for independent control of inhibitory 'noise', hence providing homeostatic regulation of the input–output function of the neurons without altering the temporal response properties of action potential-evoked synaptic transmission.

To verify that the simulation results reflect physiological conditions, we played back the inputs used for the feed-forward simulation to L2/3 pyramidal neurons of P42 NR mice after pharmacologically blocking both excitatory and inhibitory

synaptic transmission. To each neuron we played back 300 input current traces each from NR, DE and DE_{amp} conditions using a 5000-Hz eEPSC frequency, which may reflect 5000 inputs active at 1 Hz or fewer inputs at higher frequencies. To mimic the up-state used for the simulation, the cells were depolarized to 5 mV below spiking threshold during the input playback (figure 5*d*). While the DE group responded similarly to NR, the DE_{amp} group showed a larger average tonic firing rate during the 100-ms stimulation when normalized to the maximum phasic rate (figure 5*e*), such that there was a significant decrease in the ratio of phasic (max) to tonic (mean) firing rate (figure 5*f*). Furthermore, the normalized firing rate of the DE_{amp} group significantly deviated from average NR values during the tonic plateau phase while the DE group on average did not (figure 5*g*). These data further support the idea that specific manipulation of mIPSC frequency better preserves the temporal profile of neuronal firing compared with alterations in mIPSC amplitude.

To examine the robustness of our model, we used the Fokker–Planck calculation to vary key parameters and network configuration. The basic conclusion that the DE condition works better than the hypothetical DE_{amp} condition at preserving the temporal profile of neural firing was robust across a physiological range of $GABA_AR$ reversal potentials (E_{Cl}) for mature neurons (less than −50 mV) [48,49] (electronic supplementary material, figure S8*a–f*). Changing the network configuration to a feedback inhibitory circuit gave qualitatively similar results to those of a feed-forward inhibitory circuit (electronic supplementary material, figure S8*g*,*h*).

4. Discussion

Our results demonstrate that sensory experience controls the frequency of action potential-independent inhibitory 'noise' without altering eIPSCs. In particular, changes in visual experience selectively altered mIPSC frequency in adult cortex during the refractory period for inhibitory synaptic plasticity [20]. Consistent with the refractory period notion, visual deprivation did not change eIPSCs or the density of inhibitory synaptic terminals. Non-genomic actions of oestrogen via ER-α also specifically reduced mIPSC frequency in adult visual cortex and DE occluded this effect, suggesting that both use the same molecular mechanisms. Furthermore, acute blockade of ER-α in visual cortex slices from DE mice reversed the decrease in mIPSCs, which suggests that DE-induced reduction in mIPSC frequency is in part mediated by acute effects of endogenous oestrogen. Therefore, specific control of mIPSC frequency seems to be a common mechanism to homeostatically adapt inhibitory synaptic transmission in adults during the refractory period. We propose that these mechanisms, which exclusively target mIPSC frequency, enable cortical circuits with feed-forward or feedback inhibition to achieve homeostatic adaptation to global changes in input activity without compromising neural response properties or probabilistic population codes.

(a) Visual experience-dependent homeostatic regulation of miniature inhibitory postsynaptic currents

We found that changes in visual experience reversibly alter mIPSC frequency even in mature cortex during the refractory period for plasticity (figure 1; electronic supplementary material, figure S1). The polarity of these changes is consistent with homeostatic adaptation, such that lack of vision reduces the overall tone of inhibition while restoring vision increases it. L2/3 pyramidal neurons also homeostatically adjust their excitatory synaptic gain with changes in visual experience, which occurs predominantly by bidirectional regulation of the amplitude of mEPSCs [17,22–24,42,43]. The coordinated change in both mIPSC frequency and mEPSC amplitude allows for homeostatic adaptation to changes in neural activity levels by adjusting the input–output function of a neuron (figure 5*a* and electronic supplementary material, figure S6). The regulation of mEPSCs is postsynaptic in nature, which involves changes in synaptic AMPAR content [22,43], and is accompanied by alterations in the eEPSC properties [22,43]. Here we find that the regulation of inhibitory synapses is different in that it is rather specific to mIPSC frequency without changes in the parameters of eIPSCs in the mature cortex. One limitation of our interpretation is that we cannot completely rule out the possibility that the mIPSC frequency changes we observe here are due to changes in eIPSC parameters of other subtypes of perisomatic inhibitory interneurons, such as cholecystokinin (CCK)-positive neurons. However, considering that these are very small subpopulation of interneurons in the visual cortex [50], we expect their contribution to be quite limited.

The specific regulation of mIPSC frequency by visual experience contrasts *in vitro* studies using neuronal cultures showing bidirectional regulation of both mIPSC amplitude and frequency with pharmacological manipulations of neural activity [51,52]. In our studies, the amplitude regulation occurred only when DE animals were re-exposed to light, and was restricted to an early developmental period [37] (electronic supplementary material, figures S1 and S2). The apparent discrepancy may be due to several factors. Applying tetrodotoxin (TTX) to cultured neurons is expected to block all activity, including spontaneous action potentials. On the other hand, visual deprivation will leave spontaneous firing and intracortical activity intact, but only remove visually driven patterned activity. Also, *in vitro* studies are done in relatively young cultured neurons, hence they would be in the age range in which postsynaptic regulation of $GABA_ARs$ is possible [37] (electronic supplementary material, figures S1 and S2). We recently reported that once the developmental switch in $GABA_AR$ properties occurs the receptors are no longer regulated by neural activity [37] (electronic supplementary material, figure S1). At the age when postsynaptic $GABA_ARs$ are malleable, changes occurred through altering the number of receptors rather than their conductance [37] (electronic supplementary material, figure S1*c*,*d*). This is also seen from *in vitro* studies [51,52], suggesting that the main postsynaptic mode of inhibitory synapse regulation is via controlling the number of $GABA_ARs$. Furthermore, the advantage of regulating mIPSC frequency is probably only relevant for mature circuits, because there was no advantage of regulating mIPSC frequency over mIPSC amplitude when $GABA_AR$ reversal potential is depolarizing (electronic supplementary material, figure S8), as found in immature neurons [48,49]. Our simulation results also suggest that the specific regulation of mIPSC frequency is probably only relevant for conserving neuronal response properties in the context of a feed-forward (figure 5; electronic supplementary material, figure S8*a–d*) or feedback (electronic supplementary material, figure S8*g*,*h*) inhibitory circuit with high input activity. Indeed, in single neuron simulations, both mIPSC amplitude and frequency regulation

produced identical changes in neuronal input–output function (electronic supplementary material, figure S6) as well as in their ability to preserve the variance of synaptic inputs (electronic supplementary material, figure S5).

(b) Potential substrates for independent regulation of miniature inhibitory postsynaptic currents

The selective regulation of mIPSC frequency, without changes in presynaptic parameters of eIPSC, is in line with recent findings that mIPSCs and eIPSCs use distinct vesicle pools [4–9,11,13]. Presynaptic neurotransmitter vesicles are known to reside in discrete pools [53,54]: (i) a readily releasable pool (RRP) that contains docked vesicles ready for release by an action potential, (ii) a reserve pool that is recruited to RRP following extensive stimulation and (iii) a resting pool that does not undergo release even with extensive stimulation. There is evidence that spontaneous release draws specifically from the resting pool, which may be distinct from the evoked release pool [5,9], or have some degree of overlap with vesicles in the evoked release pool [10,11]. Recent studies report that the molecular release machinery for action potential-independent release is distinct from that used for evoked release. For example, VAMP7, a tetanus toxin insensitive v-SNARE, is preferentially targeted to the resting pool of vesicles [11]. There are also vesicle proteins that specifically regulate mIPSCs independent of eIPSCs. One of these is synaptotagmin-12 (Syt12), a member of the synaptotagmin family of synaptic vesicle proteins, which specifically increases mIPSC frequency without changes in eIPSC parameters [13]. Doc2b, a vesicle-associated soluble protein, has also been shown to be specifically involved in maintaining mIPSC frequency [6,12] without effects on postsynaptic mIPSC parameters or eIPSCs [6]. These findings provide potential molecular substrates through which spontaneous inhibitory neurotransmission can be regulated independent of eIPSCs. Whether and how these molecules are regulated by experience is currently unknown. A recent study showed that phosphorylation of complexin is required for selective control of spontaneous release by activity at the *Drosophila* neuromuscular junction [55], which indicates that activity-dependent regulation of spontaneous release machinery is possible.

(c) Acute oestrogen selectively alters miniature inhibitory postsynaptic current frequency

We found that oestrogen acting mainly on ER-α specifically reduces mIPSC frequency without altering eIPSC parameters in adult V1, which was occluded in DE mice. In addition, acute application of ER-α antagonist readily reversed the effects of DE. These effects were very rapidly induced with only a few minutes of acute application of E2 or ER-α agonist/antagonist, hence are likely mediated by non-genomic actions of oestrogen. Recently, studies showed that oestrogen receptors are localized on presynaptic vesicles and specifically, ER-α is associated with GABAergic vesicles [41,56]. Acute E2 application has been shown to depalmitoylate ER-α to dissociate it from presynaptic vesicles [41]. Hence, this form of non-genomic action of E2 may underlie the regulation of mIPSCs in adult V1. The rapid action of E2 and ER-α agonist/antagonist is likely due to both the lipophilic nature of these compounds, which allows them to cross the membranes easily, and the fact that they may act directly on oestrogen receptors present on presynaptic boutons [41,56]. Our observation of a rather specific regulation of mIPSC frequency by E2 is different from what is reported in hippocampal neurons. In particular, E2 reduces eIPSCs in CA1 neurons via mGluR1-dependent synthesis of endocannabinoids, which act retrogradely on CB1 receptors to reduce action potential-dependent release of GABA [39]. This effect, however, was specific to females, and not observed in males. Our results are obtained from male mice, and E2 lacked any effect on eIPSCs (figure 3). Therefore, we believe the action of E2 in adult V1 is either distinct from that seen in the hippocampus or may exhibit sex differences. While the majority of studies on oestrogen are done in females, there is evidence that neurons in the male brain can synthesize E2 from endogenous cholesterol [57]. Our data from adult male mice corroborate that DE may increase endogenous E2 to acutely reduce mIPSC frequency (figure 4). Hence, it is possible that experience-dependent regulation of mIPSCs may be mediated by local synthesis of E2 acting on ER-α present on presynaptic GABAergic vesicles in the resting pool for specific spontaneous release.

(d) Functional consequences of specifically regulating miniature inhibitory postsynaptic currents

It is well documented that the maturation of eIPSCs is experience-dependent [3]. Visual experience accelerates development, but visual deprivation beyond the early developmental period does not reverse the increase in eIPSC amplitude and release probability [25,35,36]. This is attributed to the refractory period for eIPSC plasticity following the closure of the critical period [20]. Our results are in line with these previous findings, where one week of DE does not alter any of the uIPSC or maximal eIPSC parameters measured in adults (figure 2). Therefore, experience-dependent regulation of mIPSC frequency is so far the only mechanism engaged for adjusting inhibitory tone in the mature cortex during the refractory period. One of the main functions of inhibitory interneurons, especially fast-spiking PV neurons, is to constrain the timing of input locked to presynaptic action potentials [14,15]. Additionally, in sensory cortices, inhibition plays a critical role in shaping neuronal receptive field properties [58]. Hence, changes in eIPSCs in a mature circuit may disrupt proper sensory processing. Our simulation results support this idea (figure 5). By specifically regulating mIPSC release, homeostatic control of overall neural activity may be achieved without compromising information processing, which may be especially relevant during the refractory period for eIPSC plasticity [20]. In sum, our results reveal that inhibitory 'noise' is not likely errors of the release machinery, but a critical substrate for controlling network activity in the adult cortex.

Ethics. All animal procedures were approved by the Institutional Animal Care and Use Committee (IACUC) of the University of Maryland and the Johns Hopkins University, and followed the guidelines of the National Institutes of Health (NIH).

Data accessibility. All experimental data and codes used for simulations are readily available by requesting the materials from the corresponding authors. The datasets supporting this article have been uploaded as part of the electronic supplementary material.

Authors' contributions. Electrophysiological recordings were done by M.G. (mIPSCs and eIPSCs), J.L.W. (oestrogen), S.H. (uIPSCs and feed-forward) and H.-K.L. (feed-forward). A.L. conducted GAD65 immunohistochemistry. S.M. ran the computational analyses. Data analyses were done by all authors. H.-K.L., S.M. and A.K. wrote the manuscript with the help of M.G., J.L.W. and S.H. S.M., A.K.

and H.-K.L. conceived and designed the experiments/simulations with the help of all authors.

Competing interests. We have no competing interests.

Funding. This work was supported by the National Institutes of Health (NIH) grants R01-EY012124 to A.K. and R01-EY014882 to H.-K.L. and the Howard Hughes Medical Institute (HHMI) Undergraduate Research Fellowship to A.L.

References

1. Woo RS *et al.* 2007 Neuregulin-1 enhances depolarization-induced GABA release. *Neuron* **54**, 599–610. (doi:10.1016/j.neuron.2007.04.009)
2. Tabuchi K, Blundell J, Etherton MR, Hammer RE, Liu X, Powell CM, Sudhof TC. 2007 A neuroligin-3 mutation implicated in autism increases inhibitory synaptic transmission in mice. *Science* **318**, 71–76. (doi:10.1126/science.1146221)
3. Jiang B, Huang ZJ, Morales B, Kirkwood A. 2005 Maturation of GABAergic transmission and the timing of plasticity in visual cortex. *Brain Res. Rev.* **50**, 126–133. (doi:10.1016/j.brainresrev.2005.05.007)
4. Hablitz JJ, Mathew SS, Pozzo-Miller L. 2009 GABA vesicles at synapses: are there 2 distinct pools? *Neuroscientist* **15**, 218–224. (doi:10.1177/1073858408326431)
5. Sara Y, Virmani T, Deák F, Liu X, Kavalali ET. 2005 An isolated pool of vesicles recycles at rest and drives spontaneous neurotransmission. *Neuron* **45**, 563–573. (doi:10.1016/j.neuron.2004.12.056)
6. Pang ZP, Bacaj T, Yang X, Zhou P, Xu W, Südhof TC. 2011 Doc2 supports spontaneous synaptic transmission by a Ca^{2+}-independent mechanism. *Neuron* **70**, 244–251. (doi:10.1016/j.neuron.2011.03.011)
7. Mathew SS, Pozzo-Miller L, Hablitz JJ. 2008 Kainate modulates presynaptic GABA release from two vesicle pools. *J. Neurosci.* **28**, 725–731. (doi:10.1523/JNEUROSCI.3625-07.2008)
8. Kaeser PS, Deng L, Chávez AE, Liu X, Castillo PE, Südhof TC. 2009 ELKS2alpha/CAST deletion selectively increases neurotransmitter release at inhibitory synapses. *Neuron* **64**, 227–239. (doi:10.1016/j.neuron.2009.09.019)
9. Fredj NB, Burrone J. 2009 A resting pool of vesicles is responsible for spontaneous vesicle fusion at the synapse. *Nat. Neurosci.* **12**, 751–758. (doi:10.1038/nn.2317)
10. Melom JE, Akbergenova Y, Gavornik JP, Littleton JT. 2013 Spontaneous and evoked release are independently regulated at individual active zones. *J. Neurosci.* **33**, 17 253–17 263. (doi:10.1523/JNEUROSCI.3334-13.2013)
11. Hua Z, Leal-Ortiz S, Foss SM, Waites CL, Garner CC, Voglmaier SM, Edwards RH. 2011 v-SNARE composition distinguishes synaptic vesicle pools. *Neuron* **71**, 474–487. (doi:10.1016/j.neuron.2011.06.010)
12. Groffen AJ *et al.* 2010 Doc2b is a high-affinity Ca^{2+} sensor for spontaneous neurotransmitter release. *Science* **327**, 1614–1618. (doi:10.1126/science.1183765)
13. Maximov A, Shin O-H, Liu X, Südhof TC. 2007 Synaptotagmin-12, a synaptic vesicle phosphoprotein that modulates spontaneous neurotransmitter release. *J. Cell Biol.* **176**, 113–124. (doi:10.1083/jcb.200607021)
14. Cruikshank SJ, Lewis TJ, Connors BW. 2007 Synaptic basis for intense thalamocortical activation of feedforward inhibitory cells in neocortex. *Nat. Neurosci.* **10**, 462–468. (doi:10.1038/nn1861)
15. Zhang LI, Zhou Y, Tao HW. 2011 Perspectives on: information and coding in mammalian sensory physiology: inhibitory synaptic mechanisms underlying functional diversity in auditory cortex. *J. Gen. Physiol.* **138**, 311–320. (doi:10.1085/jgp.201110650)
16. Kuhlman SJ, Lu J, Lazarus MS, Huang ZJ. 2010 Maturation of GABAergic inhibition promotes strengthening of temporally coherent inputs among convergent pathways. *PLoS Comput. Biol.* **6**, e1000797. (doi:10.1371/journal.pcbi.1000797)
17. Gao M, Sossa K, Song L, Errington L, Cummings L, Hwang H, Kuhl D, Worley P, Lee HK. 2010 A specific requirement of Arc/Arg3.1 for visual experience-induced homeostatic synaptic plasticity in mouse primary visual cortex. *J. Neurosci.* **30**, 7168–7178. (doi:10.1523/JNEUROSCI.1067-10.2010)
18. Otis TS, Staley KJ, Mody I. 1991 Perpetual inhibitory activity in mammalian brain slices generated by spontaneous GABA release. *Brain Res.* **545**, 142–150. (doi:10.1016/0006-8993(91)91280-E)
19. Blue ME, Parnavelas JG. 1983 The formation and maturation of synapses in the visual cortex of the rat. II. Quantitative analysis. *J. Neurocytol.* **12**, 697–712. (doi:10.1007/BF01181531)
20. Huang S, Gu Y, Quinlan EM, Kirkwood A. 2010 A refractory period for rejuvenating GABAergic synaptic transmission and ocular dominance plasticity with dark exposure. *J. Neurosci.* **30**, 16 636–16 642. (doi:10.1523/JNEUROSCI.4384-10.2010)
21. Ma WJ, Beck JM, Latham PE, Pouget A. 2006 Bayesian inference with probabilistic population codes. *Nat. Neurosci.* **9**, 1432–1438. (doi:10.1038/nn1790)
22. Goel A, Jiang B, Xu LW, Song L, Kirkwood A, Lee H-K. 2006 Cross-modal regulation of synaptic AMPA receptors in primary sensory cortices by visual experience. *Nat. Neurosci.* **9**, 1001–1003. (doi:10.1038/nn1725)
23. Goel A, Lee H-K. 2007 Persistence of experience-induced homeostatic synaptic plasticity through adulthood in superficial layers of mouse visual cortex. *J. Neurosci.* **27**, 6692–6700. (doi:10.1523/JNEUROSCI.5038-06.2007)
24. He K, Petrus E, Gammon N, Lee H-K. 2012 Distinct sensory requirements for unimodal and cross-modal homeostatic synaptic plasticity. *J. Neurosci.* **32**, 8469–8474. (doi:10.1523/JNEUROSCI.1424-12.2012)
25. Morales B, Choi SY, Kirkwood A. 2002 Dark rearing alters the development of GABAergic transmission in visual cortex. *J. Neurosci.* **22**, 8084–8090
26. Di Cristo G, Wu C, Chattopadhyaya B, Ango F, Knott G, Welker E, Svoboda K, Huang ZJ. 2004 Subcellular domain-restricted GABAergic innervation in primary visual cortex in the absence of sensory and thalamic inputs. *Nat. Neurosci.* **7**, 1184–1186. (doi:10.1038/nn1334)
27. Iyer R, Menon V, Buice M, Koch C, Mihalas S. 2013 The influence of synaptic weight distribution on neuronal population dynamics. *PLoS Comput. Biol.* **9**, e1003248. (doi:10.1371/journal.pcbi.1003248)
28. Richardson MJE, Gerstner W. 2005 Synaptic shot noise and conductance fluctuations affect the membrane voltage with equal significance. *Neural. Comput.* **17**, 923–947. (doi:10.1162/0899766053429444)
29. Zheng K *et al.* 2011 TrkB signaling in parvalbumin-positive interneurons is critical for gamma-band network synchronization in hippocampus. *Proc. Natl Acad. Sci. USA* **108**, 17 201–17 206. (doi:10.1073/pnas.1114241108)
30. Feldmeyer D, Lübke J, Silver RA, Sakmann B. 2002 Synaptic connections between layer 4 spiny neurone-layer 2/3 pyramidal cell pairs in juvenile rat barrel cortex: physiology and anatomy of interlaminar signalling within a cortical column. *J. Physiol.* **538**, 803–822. (doi:10.1113/jphysiol.2001.012959)
31. Hartman KN, Pal SK, Burrone J, Murthy VN. 2006 Activity-dependent regulation of inhibitory synaptic transmission in hippocampal neurons. *Nat. Neurosci.* **9**, 642–649. (doi:10.1038/nn1677)
32. Swanwick CC, Murthy NR, Kapur J. 2006 Activity-dependent scaling of GABAergic synapse strength is regulated by brain-derived neurotrophic factor. *Mol. Cell. Neurosci.* **31**, 481–492. (doi:10.1016/j.mcn.2005.11.002)
33. Kim J, Alger BE. 2010 Reduction in endocannabinoid tone is a homeostatic mechanism for specific inhibitory synapses. *Nat. Neurosci.* **13**, 592–600. (doi:10.1038/nn.2517)
34. Sarti F, Zhang Z, Schroeder J, Chen L. 2013 Rapid suppression of inhibitory synaptic transmission by retinoic acid. *J. Neurosci.* **33**, 11 440–11 450. (doi:10.1523/JNEUROSCI.1710-13.2013)
35. Huang ZJ, Kirkwood A, Pizzorusso T, Porciatti V, Morales B, Bear MF, Maffei L, Tonegawa S. 1999 BDNF regulates the maturation of inhibition and the critical period of plasticity in mouse visual cortex. *Cell* **98**, 739–755. (doi:10.1016/S0092-8674(00)81509-3)

36. Jiang B, Huang S, de Pasquale R, Millman D, Song L, Lee H-K, Tsumoto T, Kirkwood A. 2010 The maturation of GABAergic transmission in visual cortex requires endocannabinoid-mediated LTD of inhibitory inputs during a critical period. *Neuron* **66**, 248–259. (doi:10.1016/j.neuron.2010.03.021)
37. Gao M, Maynard KR, Chokshi V, Song L, Jacobs C, Wang H, Tran T, Martinowich K, Lee H-K. 2014 Rebound potentiation of inhibition in juvenile visual cortex requires vision-induced BDNF expression. *J. Neurosci.* **34**, 10 770–10 779. (doi:10.1523/JNEUROSCI.5454-13.2014)
38. Jiang B, Sohya K, Sarihi A, Yanagawa Y, Tsumoto T. 2010 Laminar-specific maturation of GABAergic transmission and susceptibility to visual deprivation are related to endocannabinoid sensitivity in mouse visual cortex. *J. Neurosci.* **30**, 14 261–14 272. (doi:10.1523/JNEUROSCI.2979-10.2010)
39. Huang GZ, Woolley CS. 2012 Estradiol acutely suppresses inhibition in the hippocampus through a sex-specific endocannabinoid and mGluR-dependent mechanism. *Neuron* **74**, 801–808. (doi:10.1016/j.neuron.2012.03.035)
40. Björnström L, Sjöberg M. 2005 Mechanisms of estrogen receptor signaling: convergence of genomic and nongenomic actions on target genes. *Mol. Endocrinol.* **19**, 833–842. (doi:10.1210/me.2004-0486)
41. Tabatadze N, Smejkalova T, Woolley CS. 2013 Distribution and posttranslational modification of synaptic ERalpha in the adult female rat hippocampus. *Endocrinology* **154**, 819–830. (doi:10.1210/en.2012-1870)
42. Desai NS, Cudmore RH, Nelson SB, Turrigiano GG. 2002 Critical periods for experience-dependent synaptic scaling in visual cortex. *Nat. Neurosci.* **5**, 783–789. (doi:10.1038/nn878)
43. Goel A, Xu LW, Snyder KP, Song L, Goenaga-Vazquez Y, Megill A, Takamiya K, Huganir RL, Lee H-K. 2011 Phosphorylation of AMPA receptors is required for sensory deprivation-induced homeostatic synaptic plasticity. *PLoS ONE* **6**, e18264. (doi:10.1371/journal.pone.0018264)
44. Turrigiano GG, Nelson SB. 2004 Homeostatic plasticity in the developing nervous system. *Nat. Rev. Neurosci.* **5**, 97–107. (doi:10.1038/nrn1327)
45. Hubel DH, Wiesel TN. 1959 Receptive fields of single neurones in the cat's striate cortex. *J. Physiol.* **148**, 574–591. (doi:10.1113/jphysiol.1959.sp006308)
46. Sillito AM. 1975 The contribution of inhibitory mechanisms to the receptive field properties of neurones in the striate cortex of the cat. *J. Physiol.* **250**, 305–329. (doi:10.1113/jphysiol.1975.sp011056)
47. Tan AYY, Chen Y, Scholl B, Seidemann E, Priebe NJ. 2014 Sensory stimulation shifts visual cortex from synchronous to asynchronous states. *Nature* **509**, 226–229. (doi:10.1038/nature13159)
48. Rheims S, Minlebaev M, Ivanov A, Represa A, Khazipov R, Holmes GL, Ben-Ari Y, Zilberter Y. 2008 Excitatory GABA in rodent developing neocortex in vitro. *J. Neurophysiol.* **100**, 609–619. (doi:10.1152/jn.90402.2008)
49. Ben-Ari Y. 2002 Excitatory actions of gaba during development: the nature of the nurture. *Nat. Rev. Neurosci.* **3**, 728–739. (doi:10.1038/nrn920)
50. Gonchar Y, Wang Q, Burkhalter A. 2007 Multiple distinct subtypes of GABAergic neurons in mouse visual cortex identified by triple immunostaining. *Front. Neuroanat.* **1**, 3. (doi:10.3389/neuro.05.003.2007)
51. Kilman V, van Rossum MC, Turrigiano GG. 2002 Activity deprivation reduces miniature IPSC amplitude by decreasing the number of postsynaptic GABA(A) receptors clustered at neocortical synapses. *J. Neurosci.* **22**, 1328–1337.
52. Rannals MD, Kapur J. 2011 Homeostatic strengthening of inhibitory synapses is mediated by the accumulation of GABA(A) receptors. *J. Neurosci.* **31**, 17 701–17 712. (doi:10.1523/JNEUROSCI.4476-11.2011)
53. Rizzoli SO, Betz WJ. 2005 Synaptic vesicle pools. *Nat. Rev. Neurosci.* **6**, 57–69. (doi:10.1038/nrn1583)
54. Südhof TC. 2000 The synaptic vesicle cycle revisited. *Neuron* **28**, 317–320. (doi:10.1016/S0896-6273(00)00109-4)
55. Cho RW, Buhl LK, Volfson D, Tran A, Li F, Akbergenova Y, Littleton JT. 2015 Phosphorylation of complexin by PKA regulates activity-dependent spontaneous neurotransmitter release and structural synaptic plasticity. *Neuron* **88**, 749–761. (doi:10.1016/j.neuron.2015.10.011)
56. Hart SA, Snyder MA, Smejkalova T, Woolley CS. 2007 Estrogen mobilizes a subset of estrogen receptor-alpha-immunoreactive vesicles in inhibitory presynaptic boutons in hippocampal CA1. *J. Neurosci.* **27**, 2102–2111. (doi:10.1523/JNEUROSCI.5436-06.2007)
57. Hojo Y *et al.* 2004 Adult male rat hippocampus synthesizes estradiol from pregnenolone by cytochromes P45017alpha and P450 aromatase localized in neurons. *Proc. Natl Acad. Sci. USA* **101**, 865–870. (doi:10.1073/pnas.2630225100)
58. Liu B-H, Li Y-T, Ma W-P, Pan C-J, Zhang LI, Tao HW. 2011 Broad inhibition sharpens orientation selectivity by expanding input dynamic range in mouse simple cells. *Neuron* **71**, 542–554. (doi:10.1016/j.neuron.2011.06.017)